



The use of genetic programming to develop a predictor of swash excursion on sandy beaches

Marinella Passarella¹, Evan B. Goldstein², Sandro De Muro¹, Giovanni Coco³

¹Department of Chemical and Geological Sciences, Coastal and Marine Geomorphology Group (CMGG), Università degli Studi di Cagliari, 09124 Cagliari, Italy

²Department of Geological Sciences, University of North Carolina, 27599, U.S.A.

³School of Environment, Faculty of Science, University of Auckland, Auckland, 1142, New Zealand

Correspondence to: Marinella Passarella (marinella.passarella@unica.it)

Abstract

We use Genetic Programming (GP), a type of Machine Learning (ML) approach, to predict the total and infragravity swash excursion using previously published datasets that have been used extensively in swash prediction studies. Three previously published works with a range of new conditions are added to this dataset to extend the range of measured swash conditions. Using this newly compiled dataset we demonstrate that a ML approach can reduce the prediction errors compared to well-established parameterizations and therefore it contributes to the error in coastal hazards assessment (e.g. coastal inundation). Predictors obtained using GP can also be physically sound and replicate the functionality and dependencies of previous published formulas. Overall, we show that ML techniques are capable of both improving predictability (compared to classical regression approaches) and providing physical insight into coastal processes.

1. Introduction

Wave runup, is the final expression of waves travelling from deep to shallow water and is directly associated to coastal hazards like flooding or erosion. Wave runup height can be defined from water level elevation time series at the shoreline $\eta(t)$, as the sum of two distinguished components: the wave set up (the temporal mean of the time series $\langle \eta \rangle$ relative to the still water level) and the swash $\eta'(t)$ (the vertical fluctuation of the water level around the wave set up). Understanding and predicting swash characteristics is critical for researchers seeking to understand the dynamics of fluid motions and sediment transport in the swash zone (e.g., Elfrink and Baldock, 2002; Masselink and Puleo, 2006), and for managers and practitioners addressing hazard setbacks, risk and coastal vulnerability (e.g., Bosom and Jimenez, 2011; Vousdoukas et al., 2012). Wave runup, (and therefore swash excursion) is a key component to evaluate inundation hazards and vulnerability to storm impacts (e.g., Bosom and Jiménez, 2011; Stockdon et al, 2007; Serafin et al., 2017). Stockdon et al., (2007) found that the wave action counted for about 48 % of the maximum total water level during two hurricanes along USA coast. The problem of



30 accurate predictions of wave runup and swash on sandy beaches has been a research topic for over 50 years but today we still struggle to provide reliable quantitative predictions.

The first predictors of wave runup were developed in the context of coastal structures (Miche, 1951; Hunt, 1959) and the formulas proposed, usually developed for steep slopes and under the assumption that runup motions reflect the standing component of the incident wave field. Overall these formulas suggested a dependence of the uprush elevation on wave steepness and structure slope. A variety of predictors have since then been developed for vertical runup (R) and swash (S) on sandy beaches (e.g. Guza and Thornton, 1982; Holman and Sallenger 1985; Holman 1986; Ruessink et al., 1998, Stockdon et al., 2006), with details of the parameterizations depending on different combinations of deep water significant wave height (H_{s0}), deep water wave length (L_0) and beach slope (β). Guza and Thornton (1982) proposed a linear relationship between the significant runup (R_s) and H_{s0} :

$$40 \quad R_s = c H_{s0} , \quad (1)$$

where $c = 0.7$. Guza and Thornton (1982) also first distinguished between infragravity and incident swash components, indicating that the swash component related to low frequencies (infragravity, R_{Ilg}) depends only on significant wave height (therefore excluding the beach slope) while the incident component can saturate as a result of the dissipative processes occurring in the surf zone. Their findings were later confirmed by several other studies although different dependencies on environmental parameters were suggested (e.g. Holman and Sallenger, 1985; Ruessink et al., 1998).

Holman and Sallenger (1985) studying an intermediate to reflective beach (Duck, North Carolina, USA) described R_s as:

$$R_s = c \xi_0 H_{s0}, \quad (2)$$

where c is a constant, H_{s0}/L_0 is the wave steepness and

$$50 \quad \xi_0 = \frac{\tan\beta}{\sqrt{H_{s0}/L_0}} \quad (3)$$

where β is the foreshore beach slope and ξ_0 is the surf similarity index which is also often used for beach classification — beaches are classified as dissipative for values of $\xi_0 < 0.23$, reflective for $\xi_0 > 1$ and intermediate between the two (Short, 1999).

Stockdon et al., (2006) used 10 experiments from different locations to generate new parameterizations of wave runup on natural beaches. The 2% exceedance value of wave runup R_2 was defined as:

$$R_2 = 1.1 \left(\langle \eta \rangle + \frac{S_{Tot}}{2} \right), \quad (4)$$

where $\langle \eta \rangle$ is the maximum setup elevation and S_{Tot} is the total swash defined as:



$$S_{Tot} = \sqrt{(S_{in})^2 + (S_{Ig})^2}, \quad (5)$$

where S_{in} and S_{Ig} are the incident and infragravity components of swash. Stockdon et al. (2006) used regression techniques to
60 obtain relationships for S_{in} and S_{Ig} :

$$S_{in} = 0.75\beta\sqrt{H_0L_0}, \quad (6)$$

and

$$S_{Ig} = 0.06\sqrt{H_0L_0}. \quad (7)$$

Stockdon et al., (2006) is the most commonly used empirical parameterization of runup but, as can be noted
65 comparing eq. 6 and 7, the beach slope is missing from the predictor of the infragravity component of swash. The
dependency (or not) of S_{Ig} on beach slope is a topic that has been debated but not solved and some authors (e.g., Ruessink et
al., 1998) have indicated that infragravity swash is independent from the beach slope while a weak dependence on beach
slope has instead been reported by others (e.g., Ruggiero et al., 2004). Cohn and Ruggiero, (2016) suggested a bathymetric
control of the infragravity swash component through 1D and 2D numerical simulations performed using Xbeach (where
70 incident swash contribution is excluded) and compared them with previous formulas (Ruggiero et al., 2001; Stockdon et al.,
2006) and field data on dissipative beaches. They suggested that beach morphology (> -2 m MSL) influences the infragravity
component of runup more than the nearshore morphology (< -2 m MSL) and indicated that including the foreshore beach
slope in the formulation of S_{Ig} improves predictability. Overall, it remains unclear if and when S_{Ig} depends on beach slope.
Finally, a number of other studies have also proposed other predictors that introduce other parameters to account for the
75 cross-shore wind component and the tidal range (Vousdoukas et al., 2012), the presence of nearshore sandbars (Cox et al.,
2013) or the sediment mean grain size for the case of gravel beaches (Poate et al., 2016). The above-mentioned empirical
runup formulas have been developed primarily with classic regression approaches (e.g.; Ruessink et al., 1998; Ruggiero et
al., 2001; Stockdon et al., 2006; Vousdoukas et al., 2012).

Because of the importance of accurate predictions of swash excursion, the predictors provided by Stockdon et al.,
80 (2006) have been tested by various authors on beaches ranging from reflective to dissipative (e.g., Vousdoukas et al., 2012;
Cohn and Ruggiero, 2016; Atkinson et al., 2017). Predictions using Stockdon et al. (2006) are certainly sound (especially
considering the task of generating a universal formula for vertical swash excursion) even though differences between
measurements and predictions, possibly associated to local conditions, are inevitably found. More importantly, the regression
approach of multiple datasets first proposed by Stockdon et al. (2006) paves the way for our working hypothesis: can
85 powerful data-driven techniques be used to provide robust, reliable and realistic predictions of swash excursion?

When enough data exists, Machine Learning (ML) is a viable approach to regression problems. ML is a sub-
discipline of computer science focused on techniques that allow computers to find insightful relationships between variables
involved in swash processes, learning at each iteration (algorithm training and validation) from the provided dataset. A key



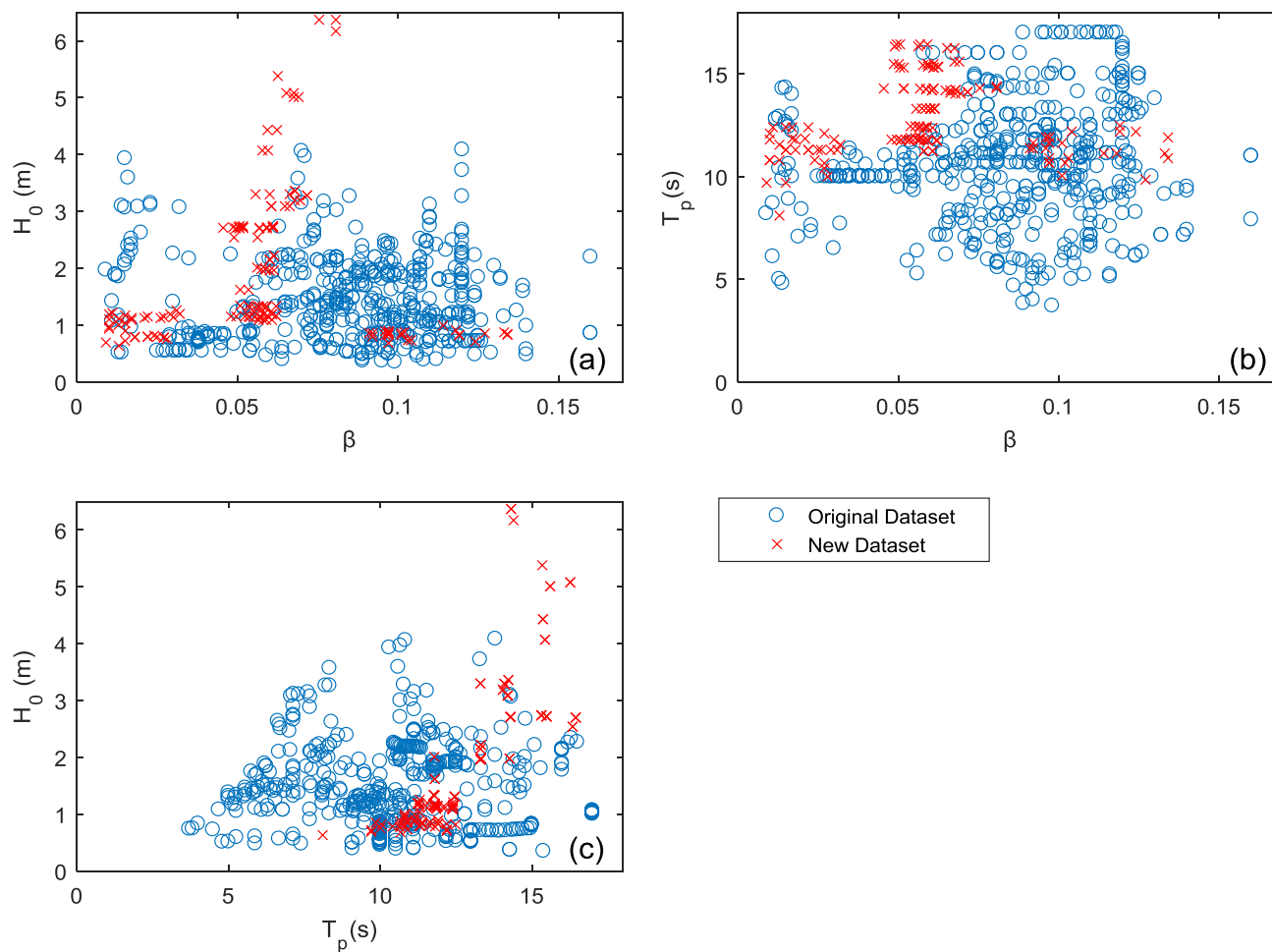
goal of ML is to develop predictors that are generalizable (able to describe the physical process beyond the training dataset
90 itself). Many different data-driven techniques fall under the purview of Machine Learning (e.g., decision trees, artificial
neural networks, Bayesian networks, and evolutionary computation), all of which have shown applicability in coastal
settings (e.g., Pape et al., 2007; Knaapen and Hulscher, 2002; Dickson and Perry, 2015; Yates and Le Cozannet, 2012).
Previous Machine Learning work has focused on predicting runup and swash, but only for engineered structures,
impermeable slopes, and/or for laboratory experiments (e.g., Kazeminezhad and Etemad-Shahidi, 2015; Bonakdar and
95 Etemad-Shahidi, 2011; Bakhtyar et al., 2008; Abolfathi et al., 2016) and not on natural beaches. In this study we focus on the
use an evolutionary technique, Genetic Programming (GP), to solve the symbolic regression problem of developing new,
optimized swash predictors.

In this contribution we first develop a swash excursion predictor using the original dataset of Stockdon et al.,
(2006), one of the most comprehensive studies in this area of research. In addition, we use data from Guedes et al., (2013),
100 Guedes et al., (2011, 2012), and Senechal, et al., (2011) to broaden the parameter space and to test the new swash equations.
The data used in this work cover a broad range of swash excursion including extreme wave conditions (maximum $H_0=6.4$ m
in Senechal, et al., 2011). High swash excursions, generated by extreme storms, are of particular interest when studying
coastal hazards because they relate to flooding, beach and dune erosion (Bosom and Jimenez, 2011; Stockdon et al., 2007).
The new ML derived results are also compared to the most widely used predictors from Stockdon et al., (2006). Finally, we
105 discuss the physical interpretation of the GP predictors and how we can use ML to gain knowledge of physical process
related to the infragravity swash component.

2 Data

This work is based on two published video image-derived runup datasets — 13 field experiments in total. The first dataset
(referred to here as the “original dataset”) is composed by 491 swash measurements from 10 experiments aggregated by
110 Stockdon et al., (2006). The second dataset (referred to here as the “new dataset”) consists of 145 swash measurements
compiled for this work from three experiments performed by Guedes et al., (2013), Guedes et al., (2011), and Senechal, et
al., (2011).

The compiled dataset of total swash is plotted in Fig. 1. The compilation of a large dataset deriving from 13
different experiments requires merging data collected using different techniques and equipment. Details of each experiment
115 can be found in the original references. Looking at the environmental forcing conditions, Figure 1 shows that the original
and new dataset cover similar ranges of beach slope, while they differ in significant wave height (the new dataset includes
wave heights over 6 m) and peak period (the original dataset includes more short period waves).



120 **Figure 1: Environmental forcing conditions (blue circles: original dataset, red crosses: new dataset): (a) significant wave height versus beach slope; (b) wave peak period versus beach slope; (c) significant wave height versus wave peak period.**

Both datasets include recordings of infragravity swash (S_{Ig} ; m), total swash (S_{Tot} ; m), beach slope (β) and concomitant offshore wave characteristics: significant wave height (H_0 ; m) and peak period (T_p ; s). From these measurements the
 125 offshore significant wave length (L_0 ; m), wave steepness (H_0/L_0), and Iribarren number (ξ_0) were calculated. Experiments were located in North America, Europe and Oceania and cover a large range of the environmental condition (see Table 1 and Fig. 1).

130



Table 1: Summary of wave and beach parameters for the original and the new datasets, beach name and type (following the classification of Short, (1999) based on Iribarren number (D stands for dissipative, I intermediate and R reflective); the last two rows indicates the range of parameters of the entire two datasets. Each experiment is associated to the citation where the measurements have been originally presented. If no reference is given, the citation to consider is Stockdon et al (2006).

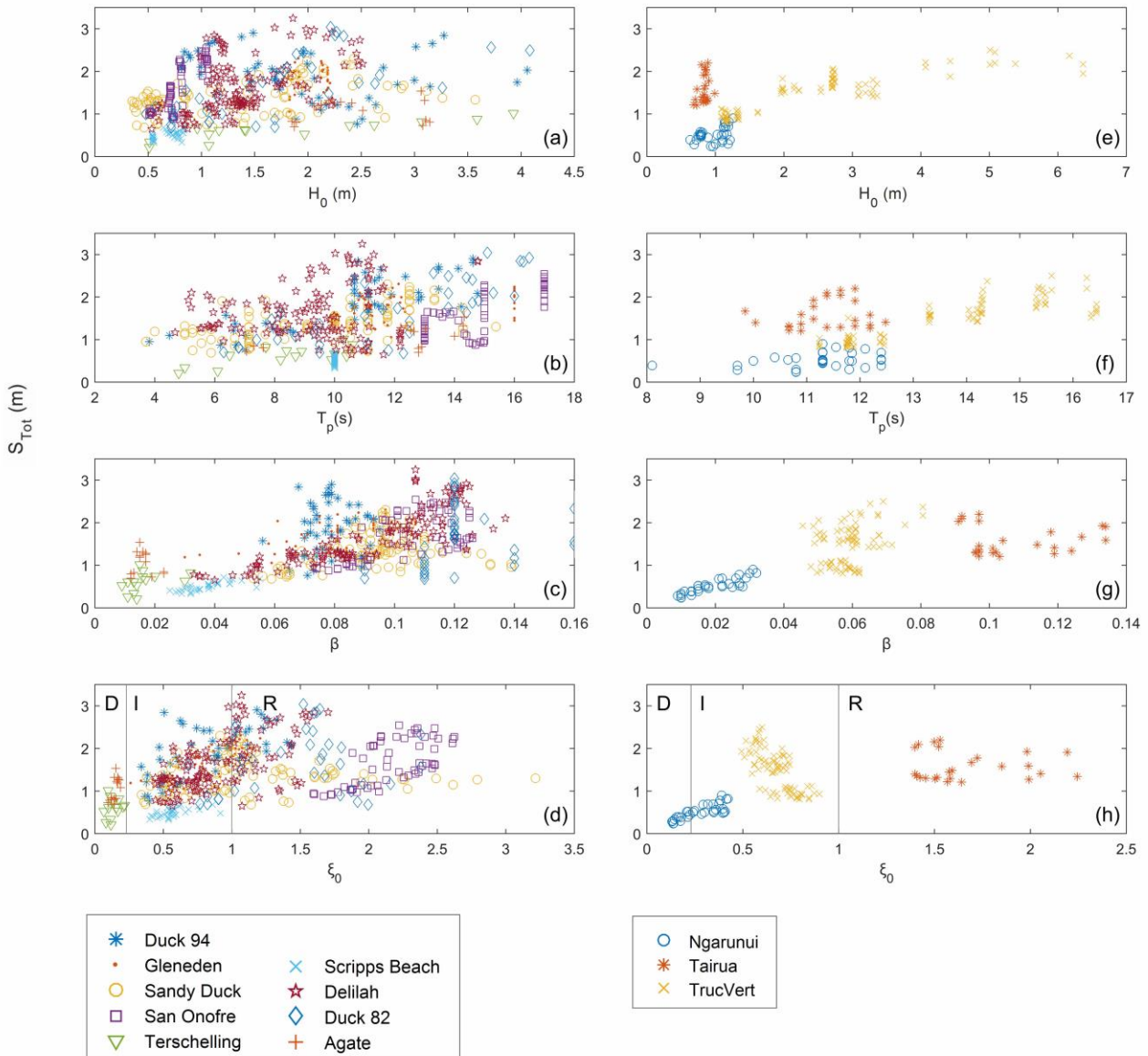
135

Experiment	Dataset (data points)	Hs (m)	Tp (s)	β	ξ_0	Beach type	S_{Tot} (m)	S_{Ig} (m)
Duck 94 (Holland and Holman, 1996)	Original (52)	0.7-4.1	3.8-14.8	0.06-0.1	0.33-1.43	I, R	0.8-2.9	0.5-2.2
Gleneden	Original (42)	1.8-2.2	10.5-16	0.03-0.11	0.26-1.2	I, R	1.1-2.3	0.9-1.9
Sandy Duck	Original (95)	0.4-3.6	3.7-15.4	0.05-0.14	0.34-3.22	I,R	0.7-2.3	0.3-1.8
San Onofre	Original (59)	0.5-1.1	13-17	0.07-0.13	1.6-2.62	R	0.9-2.6	0.5-1.8
Terschelling (Ruessink et al., 1998)	Original (14)	0.5-3.9	4.8-10.6	0.01-0.03	0.07-0.22	D	0.2-1	0.2-0.9
Scripps Beach (Holland et al., 1995)	Original (41)	0.5-0.8	10-10	0.03-0.06	0.4-0.92	I	0.3-0.7	0.3-0.7
Delilah (Holland and Holman, 1993)	Original (138)	0.5-2.5	4.7-14.8	0.03-0.14	0.44-1.70	I,R	0.7-3.3	0.4-1.7
Duck 82 (Holman, 1986)	Original (36)	0.5-4.1	6.3-16.5	0.09-0.16	0.68-2.38	I,R	0.7-3	0.4-2.4
Agate (Ruggiero et al., 2001)	Original (14)	1.8-3.1	7.1-14.3	0.01-0.02	0.1-0.19	D	0.7-1.5	0.7-1.5
Ngarunui (Guedes et al., 2013)	New (32)	0.6-1.26	8.1-12.4	0.01-0.03	0.13-0.42	D	0.24-0.9	0.24-0.9
Tairua (Guedes et al., 2011)	New (25)	0.7-1	9.9-12.5	0.09-0.13	1.4-2.25	R	1.2-2.2	0.6-0.95
TrucVert (Senechal, et al., 2011).	New (88)	1.1-6.4	11.2-16.4	0.05-0.08	0.49-0.9	I	0.81-2.5	0.63-2.37
All beaches	Entire Original (Stockdon et al., 2006), (491)	0.4-4.1	3.7-17	0.01-0.16	0.07-3.22	D,I,R	0.2-3.3	0.2-2.4
All beaches	Entire New (145)	0.6-6.4	8.1-16.4	0.01-0.13	0.13-2.25	D,I,R	0.24-2.5	0.24-2.37



Both datasets include all beach types, from dissipative to reflective. The two datasets also have a similar range of S_{Tot} (although the original dataset records a larger swash, 0.2-3.3 m vs. 0.24-2.5 m of the new dataset), S_{Ig} (about 0.2-2.4 m for
140 both), and β (about 0.01-0.1 for both). The two datasets differ in the range of offshore wave conditions — in the original dataset H_0 and T_p range over 0.4-4.1 (m) and 3.7-17 (s), respectively, while in the new dataset the ranges are 0.6-6.4 (m) and 8.1-16.4 (s).

The dissipative beaches of the original dataset (Fig. 2 d, h) are Terschelling and Agate, and for the new dataset Ngarunui (although, during the experiment, the beach also experienced intermediate conditions). The purely intermediate
145 beaches for the original and new dataset are Scripps and TrucVert. Some beaches of the original dataset represent both intermediate and reflective conditions: Duck 94, Gleneden, Sandy Duck, Delilah and Duck 82. San Onofre for the original and Tairua for new dataset are reflective.



150

Figure 2 Total swash dependence on the environmental variables of the original (a,b,c,d) and new (e,f,g,h) datasets. The variables displayed are: significant wave height (a,e), wave peak period (b,f), beach slope (c,g) and Iribarren number (d,h). Beaches are considered dissipative (D) for values of $\xi_0 < 0.23$, reflective (R) for $\xi_0 > 1$ and intermediate (I) between the two (Short, 1999).



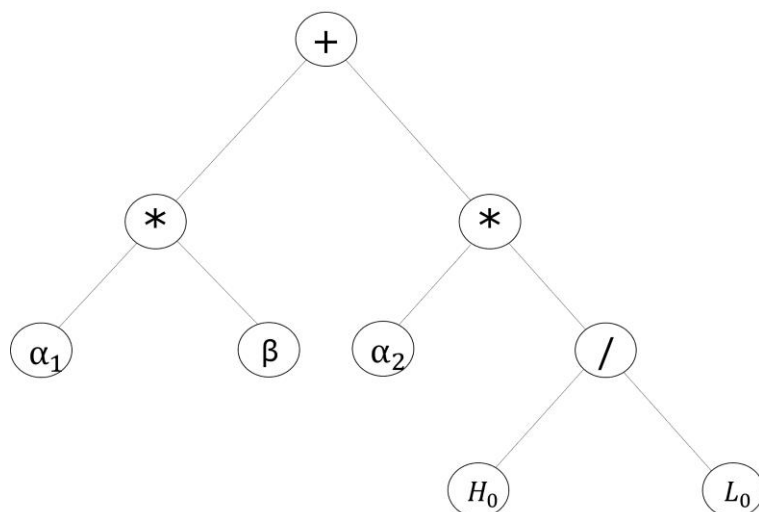
155 3. Methodology

The large amount of data available (636 field swash records), including multidimensional variables, supports the feasibility of a ML approach. The data covers a wide range of environmental conditions (including extreme storms) and beach type, ensuring the applicability of our results to sandy beaches spreading from dissipative to reflective. We now outline the methods of the study. In Sect. 3.1, we present the supervised ML approach. In Sect. 3.2 we present the data pre-processing
160 technique used to decide what data is shown to the ML algorithm. In Sect. 3.3 we discuss the techniques used to test the results from the ML algorithm against the testing data.

3.1 Genetic Programming

GP is a population-based machine learning approach based on evolutionary computation (Koza, 1992). The process of genetic programming can generally be divided into four steps: 1) an initial population of solutions for the problem is
165 produced. For regression tasks such as developing a predictor for swash, the initial population of candidate solutions is in the form of equations (encoded as a tree or graph with a predefined mix of variables, operators and coefficients; Fig. 3). For step 2 of the routine the solutions are all compared to the training data to determine ‘fitness’ using a predefined error metrics; 3) the best solutions that minimise the error are proposed and the worst solutions are discarded; 4) new solutions created through ‘evolutionary’ rules (crossover via reproduction and mutation) and are added to the population of retained solutions.
170 Steps 2 through 4 are repeated until the algorithm is stopped.

At the end of a routine, when the solutions have stabilized, a final population of solutions exist. A range of final solutions is given by the algorithm — more mathematically complex solutions (with more variables, operators, and coefficients) that minimize error are given alongside more simple, parsimonious solutions with higher error. These solutions exist along a “Pareto Front” that balances decreases in error with increasing solution complexity. Given a range of solutions
175 with different error and complexity, we do not know of a perfect method for a user to determine the single best solution from the suite of final solutions — a user must decide on the solution according to different criteria: minimization of the error, computational time, physical meaning. In our work we adopted the criteria of minimization of the error with an eye toward the ability to interpret physical meaning from the formulas. A compromise between error reduction (more complex predictors) and ability of the predictors to generalize (predictive power on new data) should be found during the selection of
180 a predictor.



$$S_{Tot} = \alpha_1 \beta + \alpha_2 \frac{H_0}{L_0}$$

Figure 3: Schematics of the GP structure and principle of operation for an example of simple total swash predictor. α_1 and α_2 are the coefficients, β , H_0 and L_0 the variables and +, * and / the mathematical operators.

185 All genetic programming in this study is performed using the software “Eureqa” developed by Schmidt and Lipson, (2009; 2013) which has successfully been used for a range of coastal problems (e.g., Goldstein et al., 2013; Tinoco et al., 2015). We searched for predictors of total and infragravity swash elevation — ultimately searching for the best equation that satisfies $S_{Tot/Ig} = f(H_0, L_0, \beta, T_p)$. Note also that we perform some experiments searching for total and infragravity swash as a function of composite variables like wave steepness, wave power (P_w), and the Iribarren number. However, the predictors
 190 did not show improvement — also keep in mind that the GP can autonomously find these interrelationships between the basic parameters themselves, leading to the appearance of these composite variables in each optimization experiment. In addition to physical parameters, constants are included in the research and the mathematical operations allowed to the GP are: addition (+), subtraction (-), multiplication (*), division (/), exponential (^) and square root ($\sqrt{\quad}$). Predictors developed on the training subset are assessed on the validation subset, using an error metric (also known as fitness function). From the
 195 available metrics we selected the mean squared error (MSE):

$$MSE = \frac{1}{N} \sum_{i=1}^N (y_i - f(x)_i)^2, \quad (8)$$

where N is the number of samples, y_i is the measured value, and $f(x)_i$ is the value predicted by GP as a function of x . The search is stopped after that 10^{11} formulas were created and evaluated by the GP process, because no significant improvement in formula performance was found.



200 All selected formulas from the genetic programming routine are further optimized. First, the formulas are rearranged algebraically to ease interpretation by the user. Second, two coefficients of each selected formula are further optimized using a gradient descent algorithm in an iterative process.

3.2 Training, Validation and Testing

205 In order to obtain generalizable predictors, it is necessary to train, validate and test any ML routine on distinct and non-overlapping subsets of data (e.g., Domingos, 2012). There is no universal, optimal method to select enough data to explain variability of the dataset while still retaining the most data to use for testing — recent work by Galelli et al., (2014) highlights that, even with the numerous input variable selection methods that have been proposed, there is no single best method for all the typologies of environmental datasets, and for all environmental models.

We adopt the maximum dissimilarity algorithm (MDA) as selection routine (e.g., Camus et al., 2011), already
210 successfully tested in other works of predictors developed by GP for physical problems (e.g., Goldstein and Coco, 2014). The MDA is a routine for the selection of the most dissimilar points in a given dataset. Each data point is a vector composed by all the variables of our data set $(\eta, S_{Tot}, S_{Ig}, S_{In}, H_0, L_0, \beta, T_p, \xi_0, P_w, R)$, where each variable is normalized between 0 and 1. At each iteration ($i=1\dots n$), the MDA finds the most different data point from the data selected in all previous iterations. Consequently the MDA selects a diverse set of data from the original 491 data points used by Stockdon et al.,
215 (2006). The operator must set the number of data points selected — we apply the MDA to 150 data points (~30% of the original dataset). We also run the analysis using a subset of variables (not including the variables representing swash elevations) but no significant loss in prediction power of the algorithms developed by the machine learning algorithm was observed). The data selected by the MDA is used as the training subset and we used the remaining data (~70 % of the original dataset, not selected) as validation subset.

220 The predictors developed by the GP using this training data was tested using the new dataset from Guedes et al., (2011), Guedes et al., (2013), and (Senechal, et al., 2011). This new dataset is completely independent from the training and unknown at the GP algorithm providing a test in the ability of the GP parameterization to generalise, even beyond the range of the testing and validation data (Fig. 1). The performance of our predictors using the testing data is compared to the Stockdon et al., (2006) predictors using the error metrics in Sect. 3.3.

225

3.3 Error Evaluation

We use three different error metrics for the testing phase and for comparing our predictor with known predictors in the literature. The mean square error as defined in Eq. (8), the root mean square error:

$$RMSE = \sqrt{\frac{1}{N} \sum_{i=1}^N (y_i - f(x)_i)^2}, \quad (9)$$



230 and the maximum absolute error:

$$MaxAE = \max_{i=1\dots N}(y_i - f(x)_i), \quad (10)$$

where N is the number of samples, y_i is the measured value, and $f(x)_i$ is the value predicted by the GP as a function of x .

4 Results

4.1 Results of GP experiments

235 After $\sim 10^{11}$ formulas were evaluated, the solutions from the GP algorithm for both S_{Tot} and S_{Ig} follow a “Pareto front” where the error decreases (compared with the validation subset) as the size (or complexity) of the formula increases. Several viable techniques exist for selecting the best solution to avoid overfitting, all meant to balance the fact that simpler solutions (the minimum description length) might risk losing more accurate information contained in more complex models (e.g., O’Neill et al., 2010). Generally, extremely complicated predictors fit the training and validation dataset better than simpler
 240 predictors but they may lose generalization power (overfitting). Picking a solution is a subjective task, and relies on specific domain knowledge on the part of the user — here we focus on predictors with clear physical plausibility (avoiding predictors with physical nonsense such as increase of S_{Tot} as H_0 decreases) and avoid predictors that are difficult to interpret, (e.g., extremely nonlinear relationships, possibly a result of overfitting the training dataset). We also focus on two predictors for both the S_{Tot} and S_{Ig} , evaluating a simpler and more complex predictor to determine if the more complex expression
 245 warrants use when generalized to the testing dataset.

4.2 Total Swash

Following the principle of error reduction and physical interpretability of the results, we finally selected from the pool of candidate solutions available from the GP experiments, two formulas for S_{Tot} , one simpler (Eq. 11) and one more elaborated (Eq. 12).

$$250 \quad S_{Tot} = 12.314 \beta + 0.087 T_p - 0.047 \frac{T_p}{H_0}, \quad (11)$$

$$S_{Tot} = 146.737 \beta^2 + \frac{T_p H_0^3}{5.800 + 10.595 H_0^3} - 4397.838 \beta^4. \quad (12)$$

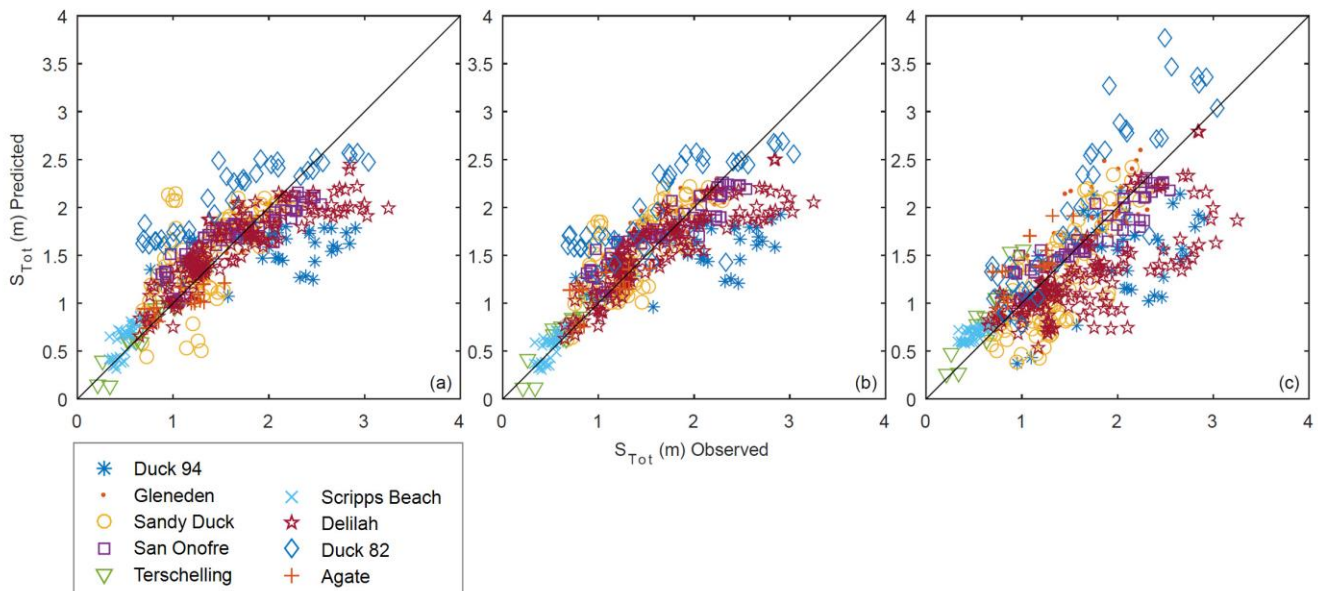
Note that the coefficients of both Eq. (11) and (12) are dimensional. Eq. (11) represents the best solution in terms of error reduction while maintaining a physical interpretability. It also stands out for its simplicity and only weak nonlinearity — it looks similar to a multiple linear regression. In Eq. 12 the first and the third term depend exclusively on β , while the
 255 second term includes the contribution of the incident waves. The total swash in both GP predictors is related to the wave peak period (instead of wave length) different from previous formulations (e.g. Stockdon et al., 2006; Holman and Sallenger 1985). Recently also Poate et al., (2016) used the wave peak period in their runup predictor for gravel beaches. The use of



the peak period instead of the wave length has no influence on the physics of the predictor, but could allow the users a more direct utilization of the formula.

260 Figure 4 displays a comparison of performance of swash predictors obtained through the ML approach (Fig. 4a, 4b) and Stockdon et al. (2006) (Fig 4c), on the training and validation dataset. This does not constitute a test of the predictors, only a consistency check to see that the predictors are modelling the training and validation data appropriately. Overall Eq. (5) shows a higher scatter in the whole original dataset (details on the errors can be found in Table 2 and Sect. 4.4). It is not clear why all formulas do not successfully fit the data Duck 82 and Delilah (especially for $S_{Tot} > 2$ m). The Stockdon et al.,
 265 (2006) predictor shows scatter at larger total swash, while the GP predictors shows slight under fitting of swash elevation during large events. Stockdon et al. (2006), Eq. (5), (6) and (7) in this contribution, mostly under predicts the data with exclusion of the Duck 82 dataset, which is largely over predicted for high values of the swash excursion. Both GP predictors more accurately fit data from dissipative beaches (Agate and Terschelling) compared with the Stockdon et al. (2006) formula.

270

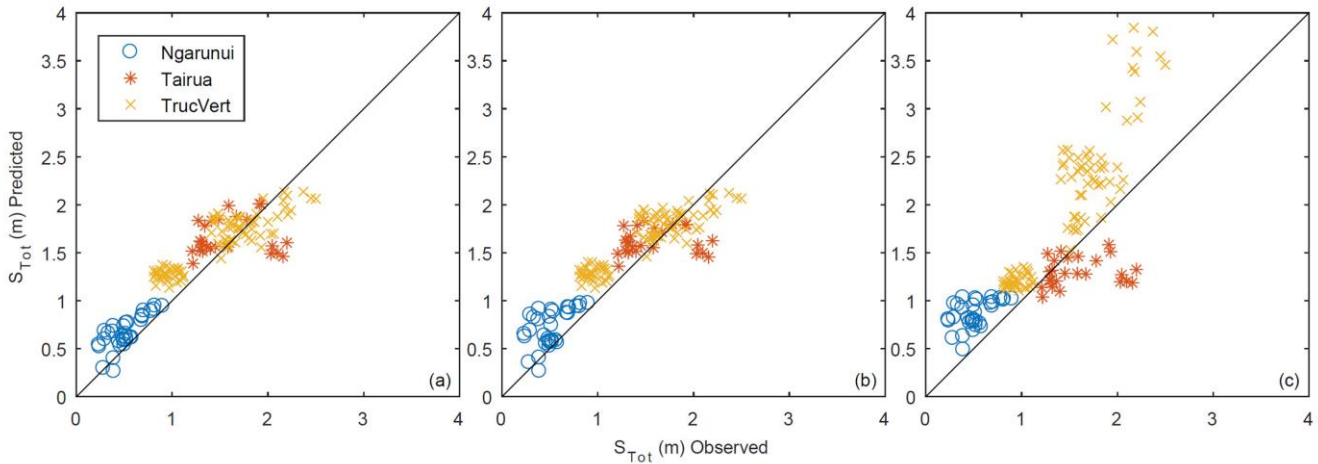


275 **Figure 4: Observed versus predicted S_{Tot} using (a) GP Eq. (11), (b) GP Eq. (12) and (c) Stockdon et al., (2006) Eq. (5) for the original dataset (Stockdon et al., 2006). This is not a test of any predictor, only a consistency check — all data was shown to the GP algorithm and used to generate the linear regression in panel c.**

Figure 5 shows the observed versus the predicted S_{Tot} — both GP models and Stockdon et al., (2006) — for the new, ‘testing’ dataset. Note that swash values (0- 2.5 m) are lower than the maxima observed in the original data set, but these values represent absolutely new, out of sample prediction for all equations. Overall the Stockdon et al., (2006) formula has higher scatter than both GP predictors (Fig. 5), and considerably overestimates swash measurement of Truc Vert



280 (intermediate beach under extreme highly energetic wave storm) and Ngarunui (dissipative beach under mild wave conditions) while underestimates the observations at the reflective beach of Tairua. Equations (11) and (12), from the GP routine, perform similarly (Fig. 5 a, b).



285 **Figure 5: Observed versus predicted S_{Tot} with the new independent dataset. (a) GP Eq. (11) , (b) GP Eq. (12) and (c) Stockdon et al., (2006) — Eq. (5) in this manuscript.**

4.3 Infragravity swash

The two formulas selected for describing S_{Ig} are Eq. (13) and the more complex Eq. (14):

$$S_{Ig} = 10\beta + \frac{\beta}{\beta - 0.306} + \frac{H_0 - 0.456}{0.447 + 136.411(\frac{H_0}{L_0})} \quad (13)$$

290
$$S_{Ig} = \frac{\beta}{0.028 + \beta} + \frac{(-1)}{2412.255\beta - 5.521\beta L_0} + \frac{H_0 - 0.711}{0.465 + 173.470(\frac{H_0}{L_0})}, \quad (14)$$

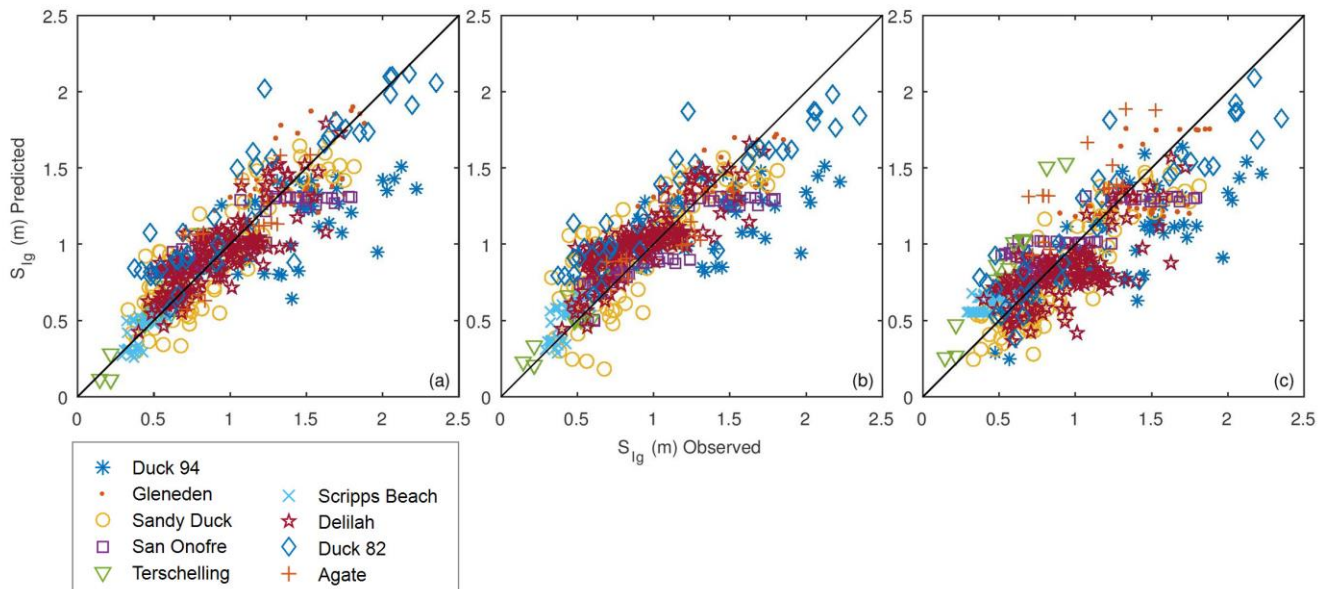
As in the case of S_{Tot} , the coefficients of Eq. (13) and (14) for S_{Ig} are dimensional. The reader should also note that both formulas depend on the beach slope in contrast with Ruessink et al., (1998) and Stockdon et al., (2006), Eq. (7) in this manuscript, but in agreement with other slope inclusive predictors (Ruggiero et al., 2001; 2004). Eq. (14) represents the best solution in terms of error reduction while maintaining physical meaning and Eq. (13) is a simpler predictor where the contribution of beach slope and waves to infragravity swash remains separate. Both Eq. (13) and (14) have the same nonlinear term $\frac{H_0 - 0.456}{0.447 + 136.411(\frac{H_0}{L_0})}$, with slight difference in the coefficients, that describes the incoming waves. The threshold

that flips this term from negative to positive is related to wave height and is probably an indication that for small waves the infragravity component is extremely limited (this term needs to be negative to compensate for other terms that only depend on beach slope and provide a constant contribution). The ML predictor not only suggests that the beach slope is important



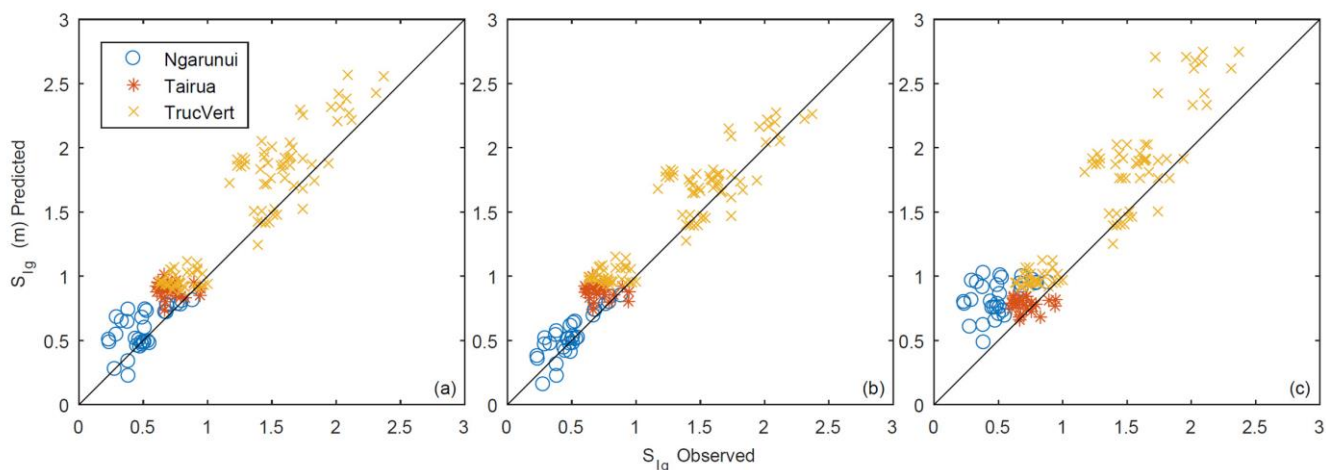
300 when predicting infragravity swash, but also indicates a nonlinear interaction between waves and beach morphology through the wave length (second term of Eq. 14).

Figure 6 displays a consistency check, highlighting the performance of swash predictors obtained through a ML approach (Fig 6a, 6b) and Stockdon et al., (2006) (Fig 6c), on the training and validation dataset. It is not clear why all formulas provide less precise prediction with data from Duck 84 and Duck 82 but we note that these two experiments focused on
 305 intermediate to reflective conditions with relatively large wave conditions (Table 1). Generally the three formulas seem to perform similarly. Some differences are found in the overestimation of Agate and Terschelling data from Stockdon et al., (2006), while the GP predictors show less scatter.



310 **Figure 6: Observed versus predicted S_{Ig} by (a) GP Eq. (13), (b) GP Eq. (14) and (c) Stockdon et al., (2006) Eq. (7) on the original dataset (Stockdon et al., 2006). This is not a test of any predictor, only a consistency check — all data was shown to the GP algorithm and is the same data used to generate the linear regression in panel c.**

The same difficulty in predicting swash excursion on a dissipative beach is observed on Ngarunui (Fig. 7). Note that this experiment was performed under mild wave conditions ($H_0 \sim 0.6-1.26$ (m) and $T_p \sim 8.1-12.4$ (s), Table 1) compared to the
 315 experiments at, Agate and Terschelling. Also Truc Vert presents dissipative conditions in the swash zone, while the surf zone is intermediate (ξ_0 up to 0.87 as reported by Senechal et al., 2011). For this experiment Eq. (13) and (7) (Fig. 7 a, c) overestimate S_{Ig} while Eq. (14) performs clearly better, suggesting that it could be the most appropriate for S_{Ig} predictions.



320 **Figure 7: Observed versus predicted S_{Ig} using (a) GP Eq. (13), (b) GP Eq. (14) and (c) Stockdon et al., (2006) Eq. (7) on the new independent dataset.**

Table 2 summarises the results of the errors calculated, through three error metrics (Sect. 3.3), of the two GP predictors and the Stockdon et al., (2006) formulas on both original and independent datasets.

325

330

335

340



Table 2: Results of error metrics for both total and infragravity swash, calculated for the GP predictors and Stockdon et al., (2006) on both original and new datasets. The results calculated with the original dataset (in Italics) do not represent a test of any predictor, only a consistency check — all original data was shown to the GP algorithm and used by Stockdon et al., (2006).

Target	Formula (Methodology)	Error Metrics	New Dataset (Independent)	Original Dataset Stockdon et al., (2006)
Total Swash	Eq. (11) (GP)	MSE (m ²)	0.074	<i>0.144</i>
		RMSE (m)	0.272	<i>0.380</i>
		MaxAE (m)	0.695	<i>1.257</i>
	Eq. (12) (GP)	MSE (m ²)	0.083	<i>0.126</i>
		RMSE (m)	0.288	<i>0.355</i>
		MaxAE (m)	0.702	<i>1.258</i>
	Eq. (5) Stockdon et al., (2006)	MSE (m ²)	0.325	<i>0.214</i>
		RMSE (m)	0.570	<i>0.462</i>
		MaxAE (m)	1.771	<i>1.399</i>
Infragravity	Eq. (13) (GP)	MSE (m ²)	0.071	<i>0.047</i>
		RMSE (m)	0.267	<i>0.217</i>
		MaxAE (m)	0.679	<i>1.019</i>
	Eq. (14) (GP)	MSE (m ²)	0.047	<i>0.053</i>
		RMSE (m)	0.216	<i>0.231</i>
		MaxAE (m)	0.587	<i>1.025</i>
	Eq. (7) Stockdon et al., (2006)	MSE (m ²)	0.111	<i>0.068</i>
		RMSE (m)	0.334	<i>0.261</i>
		MaxAE (m)	0.988	<i>1.056</i>

345 Overall the GP predictors perform better than the Stockdon et al., (2006) formulation for all the error metrics considered and for the new testing datasets (for both S_{Tot} and S_{Ig}). While for S_{Tot} the predictor of smaller size performs better than the more complex predictor, for S_{Ig} the errors decrease with increasing GP predictor size (Eq. (13) to (14)), when tested on the new dataset. Eq. (11) has the smallest RMSE (0.272 m), MSE (0.074 m²) and MaxAE (0.695 m) of the S_{Tot} formulas, evaluated on the new dataset, while the predictor from Stockdon et al. (2006) — Eq. (5) of this manuscript — has the highest RMSE

350 (0.570 m), MSE (0.325 m²) and MaxAE (1.771 m). Eq. (14) performs slightly better than Eq. (13) in predicting S_{Ig} evaluated on the new dataset, while the difference is larger when compared to the predictor from Stockdon et al. (2006) — Eq. (7) of this manuscript.



5 Discussion

In this work we use data compiled by Stockdon et al., (2006) to build new predictors, by the use of GP, for both total and
355 infragravity swash elevations. We then test the generalizability of these new predictors using new data (including some
extreme conditions). This is different from the usual use of a single dataset, divided into three parts for training, validation
and testing of ML derived predictors. We did not assume a single criteria for the selection of the best predictors, but we
found a compromise between error reduction (on the testing dataset) and the physical interpretability of the results.

Results demonstrate that the GP predictors proposed in this work perform better than existing formulas and that ML
360 can identify nonlinear relationships between the variables of this problem. Specifically, Eq. (14) introduces the dependence
of S_{I_g} on the beach slope, but also its nonlinear relationship with the wave length. Furthermore, solutions for S_{I_g} found by the
GP algorithm with the smaller size (not shown) show a simple linear dependence on H_0 with a constant (identical to early
formulation of wave runup e.g. of Guza and Thornton, 1982). More complex predictors add a dependence on L_0 , $\sqrt{H_0 L_0}$
(similar to Eq. 7 of this manuscript — from Stockdon et al., 2006) and $\frac{H_0}{L_0}$.

365 The GP algorithm found solutions for S_{I_g} that include the beach slope (β), a variable that is never excluded from
predictors of further increasing size. Because the candidate solutions resulted from GP experiments follow a “Pareto front”
distribution in which the increase in fitting (smaller MSE) grows as the size of the formula rises, the continuous inclusion of
 β for more complex predictors implies that including β in S_{I_g} formulation reduces prediction error. The improvement of
classic empirical techniques, by innovation in data-driven methodologies, has already been discussed (e.g. the case of depth-
370 averaged velocities over model vegetation by Tinoco et al., 2015). Experiments based on GP also highlighted a way to focus
on and add dependencies in predictors describing coastal processes (e.g. grain size in the case of prediction of ripple wave
length by Goldstein et al., 2013). The predictors proposed in this work perform well on a wide range on environmental
conditions, including, as defined by Nicolae et al., (2016), the highest stormy condition dataset (Truc Vert beach) recorded in
the field and available in the literature. Furthermore the work here demonstrates that ML derived results, when physically
375 plausible, may be generalizable beyond the limits of the training data, extrapolating to a novel, out of sample data set.

Looking at the limitation of the proposed models, the variables taken into account (H_0 , T_p , L_0 , β) are easily
accessible but also oversimplify the processes that affect swash. For instance, we do not include the influence of the wave
directional spread (Guza and Feddersen, 2012), the cross-shore wind component and the tidal range (Vousdoukas et al.,
2012). However, in order to include these and other aspects (e.g., role of underwater vegetation) it is necessary to perform
380 more field experiments that record swash, runup and other relevant variables. An additional limitation is that the swash
formulas obtained in this study approaches a nonzero value as wave height approaches zero. While this is physically
incorrect, the data used in the analysis does not include the limit condition of ‘no waves-no swash’. Consequently, even if
the GP formulas obtained do not correctly predict the limit condition corresponding to a no wave scenario, the prediction for
both datasets has smaller errors compared to commonly used formulas.



385 Our results contribute to the discussion on the role of beach slope on the prediction of the infragravity component of
swash. The GP algorithm found an S_{Ig} dependence on beach slope and increasingly more complicated formulas (i.e., more
precise predictions) found by the GP all include beach slope as one of the predictive variables. This result is in line with
studies such as Ruggiero et al., (2001 and 2004) and in contrast with Stockdon et al., (2006), Senechal et al. (2011) and
Ruessink et al., (1998).

390 Our results are relevant for a variety of applications where the errors related to empirical formulation obtained by
classic regression techniques could be reduced. For instance in the case of coastal hazards, Stockdon et al., (2006)
formulation for wave runup is used by Serafin and Ruggiero, (2014) for their extreme total water level estimation and by
Bosom and Jimenez, (2011) in their framework for coastal hazards assessment. Accuracy in runup formulation has
consequences for risk and vulnerability assessment as coastal management maps (De Muro et al. in press; Perini et al.,
395 2016), and other several studies regarding sediment transport (Puleo et al., 2000), swash zone hydrodynamics and
morphodynamics (Puleo and Torres-Freyermut, 2016).

6 Conclusions

Starting from a large dataset covering a wide range of swash, beach and wave field characteristics, we developed
two new predictors for total and infragravity swash elevations, using the machine learning technique of Genetic
400 Programming. We tested and compared our new formulas with previously developed and largely accepted parameterizations
of swash (e.g., Stockdon et al., 2006) using independent published datasets. Results of the two GP predictors selected (one
for total and one for infragravity swash) show better performance compared with the formulation of Stockdon et al., (2006),
evaluated using an independent (unknown to the algorithm) dataset (which included extreme highly energetic wave storm,
particularly relevant for coastal hazards). This work contributes to reducing the uncertainty in predicting the swash excursion
405 and consequently in assessing the coastal vulnerability and hazards (e.g. inundation) which depend in part upon wave swash
(Bosom and Jimenez, 2011). A better prediction of swash excursion could also influence retreat or accommodation strategies
and integrated planning for the mitigation of coastal hazards. Furthermore, GP results indicate that the beach slope
influences the infragravity component of the swash — GP predictors improve in performance when the beach slope was
included. We therefore conclude that beach slope is a relevant parameter when predicting the infragravity component of the
410 swash elevation, even though this is contrary to several previous studies (e.g., Stockdon et al., 2006; Ruessink 1998;
Senechal et al., 2011). ML and specifically GP can be a useful tool for data-rich problems providing robust predictors and
possibly also physical insight. The role and importance of the scientist is not reduced or substituted by the machine but
instead improved thanks to a powerful data analysis tool.



415 **Competing interests**

The authors declare that they have no conflict of interest.

Acknowledgments

MP gratefully acknowledges Sardinia Regional Government for the financial support of her PhD scholarship (P.O.R. Sardegna F.S.E. Operational Programme of the Autonomous Region of Sardinia, European Social Fund 2007-2013 - Axis IV
420 Human Resources, Objective 1.3, Line of Activity 1.3.1.)”. MP gratefully acknowledges the support and funding
GLOBUSDOC international placement programme of University of Cagliari. MP and SD gratefully acknowledge the
support and funding of by the Project N.E.P.T.U.N.E. (Natural Erosion Prevision Through Use of Numerical Environment)
L. R. 7.08.2007, N.7: “Promozione della ricerca scientifica in Sardegna e dell’Innovazione tecnologica in Sardegna”. GC
funded by a GNS-Hazard Platform grant (contract 3710440). EBG gratefully acknowledges the support of UoA through a
425 PBRF grant.

References

- Abolfathi, S., Yeganeh-Bakhtiary, A., Hamze-Ziabari, S. M., and Borzooei, S.: Wave runup prediction using M5’ model tree
algorithm. *Ocean Engineering*, 112, 76-81. 2016.
- 430 Atkinson, A., L., Power, H. E., Moura, T., Hammond, T., Callaghan, D. P. and Baldock, T. E. Assessment of runup
predictions by empirical models on non-truncated beaches on the south-east Australian coast. *Coastal Eng.* 119, 15-
31, doi: 10.1016/j.coastaleng.2016.10.001, 2017.
- Bakhtyar, R., Bakhtiary, A. Y., and Ghaheri, A.: Application of neuro-fuzzy approach in prediction of runup in swash
zone. *Applied Ocean Research*, 30(1), 17-27. 2008.
- 435 Bosom E., and Jiménez, J. A.: Probabilistic coastal vulnerability assessment to storms at regional scale: application to
Catalan beaches (NW Mediterranean), *Natural hazards and Earth system sciences*, 11(2), 475-84,2011.
- Bonakdar L. and Etemad-Shahidi A.: Predicting wave run-up on rubble-mound structures using M5 model tree, *Ocean Eng.*,
38, 111–118, doi:10.1016/j.oceaneng.2010.09.015, 2011.
- Camus, P., Mendez, F.J., Medina, R., and Cofino, A.S.: Analysis of clustering and selection algorithms for the study of
440 multivariate wave climate, *Coastal Eng.* 58, 53–462, doi:10.1016/j.coastaleng.2011.02.003, 2011.
- Cohn N., and Ruggiero P.: The influence of seasonal to interannual nearshore profile variability on extreme water levels:
Modeling wave runup on dissipative beaches, *Coastal Eng.* 115, 79–92, [doi:10.1016/j.coastaleng.2016.01.006](https://doi.org/10.1016/j.coastaleng.2016.01.006),
2016.



- 445 Cox, N., Dunkin, L.M., Irish, J.L.: An empirical model for infragravity swash on barred beaches. *Coast. Eng.* 81, 44–50,
doi:10.1016/j.coastaleng.2013.06.008, 2013.
- De Muro S., Ibba A., Simeone S., Buosi C. and Brambilla W. An integrated sea-land approach for mapping
geomorphological and sedimentological features in an urban microtidal wave-dominated beach: a case study from S
Sardinia, western Mediterranean. *J Maps*, in press.
- Dickson, M. E., and Perry, G. L.: Identifying the controls on coastal cliff landslides using machine-learning
450 approaches. *Environmental Modelling & Software*, 76, 117-127. 2016.
- Domingos, P.: A few useful things to know about machine learning. *Communications of the ACM*, 55(10), 78-87. 2012.
- Elfrink, B. and Baldock, T., 2002. Hydrodynamics and sediment transport in the swash zone: a review and perspectives.
Coast. Eng., 45(3), 149-167.
- Galelli, S., Humphrey, G. B., Maier, H. R., Castelletti, A., Dandy, G. C., and Gibbs, M. S.: An evaluation framework for
455 input variable selection algorithms for environmental data-driven models. *Environmental Modelling &
Software*, 62, 33-51. 2014.
- Goldstein E.B., Coco G., Murray A.B.: Prediction of wave ripple characteristics using genetic programming, *Cont. Shelf
Res.*, 71, 1–15, doi:10.1016/j.csr.2013.09.020, 2013.
- Goldstein E.B. and Coco G.: A machine learning approach for the prediction of settling velocity, *Water Resour. Res.*, 50,
460 3595–3601, doi:10.1002/2013WR015116, 2014.
- Guedes, R. M. C., Bryan, K. R., Coco, G., and Holman R. A.: The effects of tides on swash statistics on an intermediate
beach, *J. Geophys. Res.*, 116, C04008, 1-13, doi:10.1029/2010JC006660, 2011.
- Guedes, R. M. C., Bryan, K.R., and Coco, G.: Observations of alongshore variability of swash motions on an intermediate
beach, *Cont. Shelf Res.*, 48(1), 61-74, doi:10.1016/j.csr.2012.08.022, 2012.
- 465 Guedes, R. M. C., Bryan, K. R., and Coco, G.: Observations of wave energy fluxes and swash motions on a low-sloping,
dissipative beach, *J. Geophys. Res.*, 118(7), 3651-3669, doi: 10.1002/jgrc.20267, 2013.
- Guza, R.T., and Thornton E.B., Swash oscillations on a natural beach, *J. Geophys. Res.*, 87, 483-491, doi:
10.1029/JC087iC01p00483, 1982.
- Guza, R. T., and Feddersen F.: Effect of wave frequency and directional spread on shoreline runup, *Geophys. Res. Lett.*, 39,
470 L11607, doi:10.1029/2012GL051959, 2012.
- Holland, K.T., Raubenheimer, B., Guza, R.T., Holman, R.A.: Runup kinematics on a natural beach. *Journal of Geophysical
Research* 100 (C3), 4985–4993. 1995
- Holland, K.T., Holman, R.A.: Statistical distribution of swash maxima on natural beaches. *Journal of Geophysical Research*
98 (C6), 10271–10278. 1993
- 475 Holland, K.T., and Holman, R.A.: Field observations of beach cusps and swash motions. *Marine Geology* 134, 77–93. 1996
- Holman, R. A.: Extreme value statistics for wave run-up on a natural beach, *Coastal Eng.*, 9, 527–544, doi:10.1016/0378-
3839(86)90002-5, 1986.



- Holman, R. A., and Sallenger A.: Setup and swash on a natural beach, *J. Geophys. Res.*, 90(C1), 945–953, doi: 10.1029/JC090iC01p00945, 1985.
- 480 Hunt, L. A.: Design of seawalls and breakwaters. *Proc. ASCE*, 85, 123-152, 1959.
- Kazeminezhad M.H., and Etemad-Shahidi A.: A new method for the prediction of wave runup on vertical piles. *Coast. Eng.*, 98, 55–64, doi: 10.1016/j.coastaleng.2015.01.004 , 2015.
- Knaapen, M. A. F. and Hulscher, S. J. M. H. : Regeneration of sand waves after dredging, *Coast. Eng.*, 46, 277–289, doi: 10.1016/S0378-3839(02)00090-X . 2002.
- 485 Koza, J. R. *Genetic Programming, on the Programming of Computers by Means of Natural Selection*, MIT Press, Cambridge, 1992.
- Masselink, G. and Puleo, J.A.: Swash-zone morphodynamics. *Continental Shelf Research*, 26(5), 661-680. 2006.
- Miche. K.: Le pouvoir réfléchissant des ouvrages maritimes exposés a l'action de la houle, *Ann. Pours Cliaussees*, 121,285-319, 1951.
- 490 Nicolae, L.A; Pedreros, R. and Senechal, N.: Wave set-up and run-up variability on a complex barred beach during highly dissipative storm conditions. In: Vila-Concejo, A.; Bruce, E.; Kennedy, D.M., and McCarroll, R.J. (eds.), *Proceedings of the 14th International Coastal Symposium (Sydney, Australia)*. *Journal of Coastal Research*, Special Issue, 75, 882–886. Coconut Creek (Florida), ISSN 0749-0208, 2016.
- O'Neill M., Vanneschi L., Gustafson S., Banzhaf W.: Open issues in genetic programming. *Genetic Programming and Evolvable Machines*, 11, 339–363, doi: 10.1007/s10710-010-9113-2, 2010.
- 495 Pape, L., Ruessink, B. G., Wiering, M. A., and Turner, I. L.: Recurrent neural network modeling of nearshore sandbar behavior, *Neural Netw.* 20, 509–518, doi: 10.1016/j.neunet.2007.04.007, 2007.
- Perini, L., Calabrese, L., Salerno, G., Ciavola, P., and Armaroli, C.: Evaluation of coastal vulnerability to flooding: comparison of two different methodologies adopted by the Emilia Romagna region (Italy), *Nat. Hazards Earth Syst. Sci.*, 16, 181– 194, doi:10.5194/nhess-16-181-2016, 2016.
- 500 Poate, T., McCall, R., Masselink, G.: A new parameterisation for runup on gravel beaches. *Coast. Eng.* 117, 176–190, doi:10.1016/j.coastaleng.2016.08.003, 2016.
- Puleo J. A, Beach R. A., Holman R. A., and Allen J.S.: Swash zone sediment suspension and transport and the importance of bore-generated turbulence. *J. Geophys. Res.*, 105, NO C7, 17,021-17,044, doi:10.1029/2000JC900024, 2000.
- 505 Puleo J. A. and Torres-Freyermuth A.: The second international workshop on swash-zone processes. *Coastal Eng.*, 115, 1–7, doi:10.1016/j.coastaleng.2015.09.007, 2016.
- Ruessink, B. G., Kleinhans, M. G., and Van den Beukel, P. G. L.: Observations of swash under highly dissipative conditions, *J. Geophys. Res.*, 103, 3111–3118, doi:10.1029/97JC02791, 1998.
- Ruggiero, P., Komar, P. D., Marra, J. J. , McDougal, W. G. , and Beach, R. A.: Wave runup, extreme water levels and the erosion of properties backing beaches, *J. Coastal Res.*, 17, 407–419. 2001
- 510



- Ruggiero, P., Holman, R. A., and Beach, R. A.: Wave run-up on a high-energy dissipative beach, *J. Geophys. Res.*, 109, C06025, doi:10.1029/2003JC002160, 2004.
- Schmidt M, Lipson H.: Distilling free-form natural laws from experimental data. *Science.*, Apr 3;324(5923), 81-5, doi: 10.1126/science.1165893, 2009.
- 515 Schmidt, M., and Lipson H.: Eureqa (Version 1.24.0 (build 9367).) [Software], [Available at <http://www.eureqa.com/>], 2013.
- Senechal, N., Coco, G., Bryan, K.R. and Holman, R.A.: Wave runup during extreme storm conditions, *J. Geophys. Res.*, 116, C07032, doi:10.1029/2010JC006819, 2011.
- Serafin, K. A., and Ruggiero, P. Simulating extreme total water levels using a time-dependent, extreme value approach, *J. Geophys. Res.*,: Oceans, 119 (9),6305–6329, doi: 10.1002/2014JC010093, 2014.
- 520 Serafin, K. A., Ruggiero, P., Stockdon, H.: The relative contribution of waves, tides, and non-tidal residuals to extreme total water levels on US West Coast sandy beaches. *Geophys. Res. Lett.* 44, 1839–1847, doi:10.1002/2016GL071020, 2017.
- Stockdon, H. F., R. A. Holman, P. A. Howd, and A. H. Sallenger Jr.: Empirical parameterization of setup, swash and runup, *Coastal Eng.*, 53, 573–588, doi:10.1016/j.coastaleng.2005.12.005, 2006.
- 525 Stockdon, H.F. Sallenger A.H. Jr., Holman R.A., Howd P.A.: A simple model for the spatially-variable coastal response to hurricanes, *Mar. Geol.*, 238, 1-20, doi:10.1016/j.margeo.2006.11.004. 2007.
- Short, A.D. *Handbook of Beach and Shoreface Morphodynamics*. Wiley, West Sussex, England. 379, ISBN: 978-0-471-96570-1, 1999.
- Tinoco, R. O., Goldstein, E. B., and Coco, G.: A data-driven approach to develop physically sound predictors: application to depth-averaged velocities on flows through submerged arrays of rigid cylinders. *Water Resour. Res.* 51, 1247–1263, doi: 10.1002/2014WR016380, 2015.
- 530 Vousdoukas, M.I., Wziatek, D. and Almeida, L.P.: Coastal vulnerability assessment based on video wave run-up observations at a mesotidal, steep-sloped beach, *Ocean Dynam.*, 62(1), 123-137. doi:10.1007/s10236-011-0480-x, 2012.
- 535 Yates, M. L., and Le Cozannet, G.: Brief communication ‘Evaluating European coastal evolution using Bayesian networks’, *Nat. Hazards Earth Syst. Sci.* 12, 1173–1177. doi: 10.5194/nhess-12-1173-2012, 2012.